Cardiovascular Research (2009) **84**, 378–386
doi:10.1093/cvr/cvp240

# CB1 and CB2 cannabinoid receptors differentially regulate the production of reactive oxygen species by macrophages

**Ki Hoon Han[1]*†, Sunny Lim[1†], Jewon Ryu[1], Cheol-Whan Lee[1], Yuna Kim[1], Ju-Hee Kang[1], Soon-Suk Kang[2], Yeong Ki Ahn[1], Chan-Sik Park[2], and Jae Joong Kim[1]**

[1]*Division of Cardiology, Department of Internal Medicine, Asan Medical Center, University of Ulsan College of Medicine, 388-1 Pungnap-2-dong Songpa-gu, 138-736 Seoul, Republic of Korea; and* [2]*Department of Pathology, Asan Medical Center, University of Ulsan College of Medicine, Seoul, Republic of Korea*

Received 9 March 2009; revised 15 June 2009; accepted 2 July 2009; online publish-ahead-of-print 11 July 2009

**Time for primary review: 23 days**

**KEYWORDS**
CB1 receptor;
CB2 receptor;
Macrophages;
Reactive oxygen species (ROS);
Cytokines;
Rap1

**Aims** We investigated the mechanism by which cannabinoid receptors-1 (CB1) and -2 (CB2) modulate inflammatory activities of macrophages.

**Methods and results** Real-time polymerase chain reaction showed the predominant CB2 expression in freshly isolated human monocytes. PMA, a potent inducer of differentiation, upregulated CB1 and increased CB1:CB2 transcript ratio from 1:17.5 to 1:3 in 5 days of culture. Immunohistochemistry showed that CB1 protein was colocalized in CD68- and CD36-positive macrophages in human atheroma. Through selective expression of CB1 or CB2 to thioglycollate-elicited peritoneal macrophages, we proved that CB1 and CB2 mediate opposing influences on the production of reactive oxygen species (ROS). Flow cytometry showed that cannabinoid-induced ROS production by macrophages was CB1-dependent. Immunoblotting assays confirmed that macrophage CB1, not CB2, induced phosphorylation of p38-mitogen-activated protein kinase, which modulated ROS production and the subsequent synthesis of tumour necrosis factor-$\alpha$ and monocyte chemoattractant protein-1. Pull-down assays showed that the Ras family small G protein, Rap1 was activated by CB2. Dominant-negative Rap1 profoundly enhanced CB1-dependent ROS production by macrophages, suggesting CB2 Rap1-dependently inhibits CB1-stimulated ROS production.

**Conclusion** CB1 promotes pro-inflammatory responses of macrophages through ROS production, which is negatively regulated by CB2 through Rap1 activation. Blocking CB1 together with selective activation of CB2 may suppress pro-inflammatory responses of macrophages.

## 1. Introduction

Atherosclerosis exhibits features characteristic of chronic inflammatory disease.[1] At the earliest stage of atherogenesis, monocytes are recruited to the vascular wall, where they differentiate to macrophages and lipid-laden foam cells.[2] Recently, immunomodulatory effects of cannabinoids have been reported[3] and the immunosuppressive and anti-inflammatory effects of cannabinoids have been attributed to signalling mediated by the cannabinoid receptor 2 (CB2), which is mainly expressed in immune cells, including monocytes and T and B lymphocytes.[4] CB2 inhibits chemokine (CXCL12 and CXCR4)-mediated chemotaxis of Jurkat and primary human T cells.[5,6] Genetic disruption of CB2 abolishes the inhibitory effect of the cannabinoid, delta-9-tetrahydrocannabinol (THC), on the migratory capacity of thioglycollate-elicited peritoneal macrophages in response to monocyte chemoattractant protein-1 (MCP-1).[7] CB2 is also expressed in vascular smooth muscle cells (VSMCs) and endothelial cells (ECs), and attenuates TNF-$\alpha$-induced proliferation and migration of VSMCs[8] and the expression of adhesion molecules and MCP-1 by ECs.[9] A recent study demonstrated a role for CB2 in the process of atherosclerosis *in vivo*, showing that the oral administration of THC to hypercholesterolemic apoE knockout (apoE-KO) mice reduced the severity of atherosclerosis, which was blocked by administration of the selective CB2 receptor antagonist, SR144528.[7]

Recent evidence suggests that cannabinoid receptor 1 (CB1) expression is distributed beyond the central nervous system.[3] Like CB2, CB1 has been detected in VSMCs and ECs[10] and modulates blood pressure and heart rate.[3] Inflammatory cells, including human monocytes/macrophages,

* Corresponding author. Tel: +82 2 3010 3150; fax: +82 2 486 5918.
*E-mail address*: steadyhan@amc.seoul.kr
† K.H.H. and S.L. contributed equally to the work as first authors.

also express CB1, which is reportedly 10–100 times lower than that of CB2 under basal conditions.[3] Oral administration of the specific CB1 antagonist, rimonabant (SR141716; 30 mg $kg^{-1}$ $day^{-1}$ for 3 months), had shown to reduce the degree of thioglycollate-induced macrophage recruitment and the size of atheromas[11] in hypercholesterolemic low-density lipid receptor knockout (LDLR-KO) mice. However, no mechanism to explain how CB1 might affect the development of atherosclerosis had been studied.

In the present study, we investigated the functional implications of CB1 expression for the inflammatory activities of monocytes/macrophages. We found that human monocytes undergo a significant change in the CB1 and CB2 expression profile during differentiation into macrophages, with CB1 expression becoming more prominent. We also discovered that CB1 and CB2 differentially regulate macrophage activities, showing that CB1 induced the generation of reactive oxygen species (ROS) and subsequent production of pro-inflammatory cytokines by macrophages, whereas CB2 suppressed CB1-stimulated ROS production through a pathway involving the small G protein, Rap1.

## 2. Methods

### 2.1 Materials

Anandamide (AEA) was from Calbiochem (San Diego, CA, USA), and Arachidonyl-2-chloroethylamide (ACEA) and JWH015 were from Cayman chemicals (Ann Arbor, MI, USA). SR141716 (rimonabant) was obtained from Sanofi-Aventis. AM630 was purchased from Tocris. Stock solutions of AEA, ACEA, SR141716, and JWH015 were prepared in 100% ethanol. AM630 was prepared in DMSO. PDTC, PD98059, and SP600125 were from Calbiochem. SB203580 and N-acetyl-L-Cysteine (NAC) were from Sigma-Aldrich (St Louis, MO, USA).

### 2.2 Cell culture

The murine macrophage cell line, RAW264.7, was cultured in Dulbecco's modified Eagle's medium (DMEM, Invitrogen, Carlsbad, CA, USA) containing 10% foetal bovine serum, 100 μg/mL penicillin and 100 μg/mL streptomycin.

Peripheral blood mononuclear cells (PBMCs) were isolated from fresh whole blood (3–10 mL) by layering onto Picoll Hypaque (1:1 = v/v, d = 1.077 g/mL; Sigma-Aldrich), and centrifugation (600 *g*/15 min at 22°C). Human macrophages were prepared from PBMCs by plating on culture dishes and incubating in RPMI 1640 medium supplemented with 20% autologous serum and antibiotics in the presence of PMA. All human blood donors provided the informed written consent, which was reviewed and approved by Ethics Board, University of Ulsan, Korea. And the present study conforms with the principles outlined in the Declaration of Helsinki.

CB2-KO mice (C57BL/6J background) and C57BL/6J wild-type mice were purchased from the Jackson laboratory. Thioglycollate-elicited peritoneal macrophages were prepared by injecting mice intraperitoneally with 1 mL 3% thioglycollate (Sigma-Aldrich) in PBS. Intra-peritoneal cells were harvested 5 days later and allowed to adhere on 12-well plates for 2 h, and then non-adherent cells were removed by washing.

All animals were maintained under pathogen-free conditions following US National Institute of Health Guidelines. The protocol was reviewed and approved by the Animal Subjects Committee of the Asan Medical Center (Seoul, South Korea) and the present study conforms with the Guide for the Care and Use of Laboratory Animals published by the US National Institutes of Health (NIH Publication No. 85-23, revised 1996).

### 2.3 Expression constructs and transfection

Expression constructs of human CB1 (GeneBank accession no. NM_016083), CB2 (NM_001841), and Rap1 (NM_001010935) were prepared by amplifying the complete coding sequences of by polymerase chain reaction (PCR) and cloning into the pcDNA3.1 vector (Invitrogen). The expression plasmid for a dominant negative form of Rap1 (Rap1DN) was kindly provided by Dr EY Moon.[12]

RAW 264.7 cells ($2 \times 10^4$ cells/well) were transfected with Rap1DN using 0.5 μg DNA and 1.5 μL FuGENE6 reagent, as described by the manufacturer (Roche Applied science). The transfection of human CB1 or CB2 or Rap1DN into peritoneal macrophages was performed using the Effectene transfection reagent (Qiagen; DNA: DNA-condensation buffer: Enhancer: Effectene Transfection Reagent=0.3 μg:75 μL:2.4 μL:6 μL). The transfected cells were used for experiments after 24 h.

### 2.4 Analysis of mRNA expression

For conventional RT–PCR, targets were amplified from synthesized cDNA using 32 cycles of 94°C for 30 s, 58°C for 30 s, and 72°C for 2 min. The following specific primers were used: Human CB1: 5′-CTCACAGCCATCGACAGGTA-3′ (forward), 5′-CGCAGGTCCTTACTCC TCAG-3′ (reverse); Human CB2: 5′-TGCTCTGAGCTTTTCCCACT-3′ (forward), 5′-GGGCTTCTTCTTTTGCCTCT-3′ (reverse); Mouse CB1: 5′-ATCTTAGACGGCCTTGCAGA-3′ (forward), 5′-GGACTATCTTTGCGG TGGAA-3′ (reverse); Mouse CB2: 5′-AGTGTGACCATGACCTTCAC-3′ (forward), 5′-TCCAGAGGACATACCCATAG-3′ (reverse); GAPDH: 5′-G ACCCCTTCATTGACCTC-3′ (forward), 5′-GCTAAGCAGTTGGTGGTG-3′ (reverse).

Alternatively, real-time PCR was performed using a LightCycler 1.5 (Roche Diagnostics, Almere, The Netherlands) with SYBR-Green I detection. The cycling conditions consisted of 95°C for 15 s, 60°C for 5 s, and 72°C for 25 s. After 45 cycles, the melting point was determined and dissociation curves were obtained to assure the specificity of the reaction. The specific primers used were as follows: Human CB1: 5′-CAACAAGTCTCTCTCGTCCT-3′ (forward), 5′-GATGAAGTGGTAGGAAGGC-3′ (reverse); Human CB2: 5′-CACTG ATCCCCAATGACTAC-3′ (forward), 5′-CCACTCCGTAGAGCATAGAT-3′ (reverse); Human GAPDH: 5′-GACCCCTTCATTGACCTC-3′ (forward), 5′-GCTAAGCAGTTGGTGGTG-3′ (reverse).

The Ct value (i.e. the cycle number at which emitted fluorescence exceeded an automatically determined threshold) for target cDNA was corrected by the Ct value for GAPDH and expressed as ΔCt. Data are expressed as fold changes of mRNA levels, calculated using the following formula:

$$\text{Fold change} = 2^{(\Delta Ct \text{ for untreated cells} - \Delta Ct \text{ for treated cells})}.$$

### 2.5 Intracellular reactive oxygen species detection

ROS in monocytes were monitored using the fluorescent ROS indicator, C2′,7′-dichlorodihydrofluorescein diacetate ($H_2$DCFDA 5 μM; Molecular Probes) as described.[13] Cell-associated fluorescence was detected by FACS using the FACSort flow cytometer (CELLQUEST software) or by confocal microscopy using the TCS-SP2 system (Leica Microsystems Nussloch GmbH, Germany). Spontaneous photo-oxidation of cell-associated $H_2$DCFDA was minimized by collecting the fluorescent image in a single rapid scan.

### 2.6 Immunoblotting

Cell lysate (40 μg protein) in a cell lysis buffer (0.2% SDS, 5 mM EDTA, 100 mM PMSF, 2 μg/mL leupeptin, 1 μM pepstain, 2 mM benzamidine in PBS) was separated by SDS–PAGE on 12% gels, and immunoblotted as described previously[14] using specific antibodies against p38-MAPK and phospho-p38-MAPK (Cell Signaling Technology, Boston, MA, USA), and β-actin (Sigma-Aldrich). Horseradish peroxidase (HRP)-conjugated goat anti-rabbit IgG (1:20000, Jackson ImmunoResearch Lab Inc.) was used as a secondary antibody, and the blots were developed using an enhanced chemiluminescence

(ECL) kit (Amersham, Piscataway, NJ, USA). Protein was quantified by MULTI-IMAGE analysis system and Quantity One quantitation software (Bio-Rad Laboratories Inc., Hercules, CA, USA).

### 2.7 Detection of GTP-bound Rap1

The active, GTP-bound form of Rap1 was detected using an assay kit (Pierce, IL, USA). Briefly, 500 μg protein from a cell lysate was incubated with 20 μg GST-human RalGDS-RBD (Rap binding domain of RalGDS) to precipitate GTP-bound Rap1. The amount of GTP-bound Rap1 was estimated by immunoblotting, as described above, using a mouse anti-Rap1 monoclonal IgG (Pierce).

### 2.8 Detection of CB1 and CB2 in atheroma

Atherosclerotic coronary artery tissue from six male subjects with unstable angina was used for analysis of CB1 and CB2 in atheromas. An intimal portion of the atheroma was obtained by guided directional coronary atherectomy, which had to be performed prior to positioning of the metal stent. All human tissue donors provided the informed written consent, which was reviewed and approved by Ethics Board, University of Ulsan, Korea. And the present study conforms with the principles outlined in the Declaration of Helsinki. The tissue sample was immersed in isopentane solution at $-70^{\circ}$C and frozen in Jung Tissue Freezing Medium (Leica Instruments GmbH, Nussloch, Germany), after which 5 μm thick slices were obtained and mounted onto glass slides. Non-specific antibody binding was blocked by incubating sections in 5% normal swine serum (Vector Laboratories, Burlingame, CA, USA) for 30 min at room temperature. The samples were subsequently incubated with anti-CB1 (Santa Cruz; 1:150), anti-CB2 (Santa Cruz; 1:150), anti-CD36 (Dako; 1:200), or anti-CD68 (Santa Cruz; 1:100) antibodies. Tissue-bound antibody was detected by HRP-conjugated avidin biotin or alkaline phosphatase systems, which use 3,3′-diaminobenzidine (DAB) and Vector blue as substrates (Vector Laboratories Burlingame, CA, USA). All sections were lightly counterstained with Mayer's haematoxylin.

### 2.9 Measuring cytokine concentrations

Mouse peritoneal macrophages in RPMI1640 or RAW 264.7 cells in DMEM ($2 \times 10^4$ cells/well) were seeded onto 12-well plates and the concentrations of TNF-α, MCP-1, IFNγ, IL-1α, IL-6, and IL-12 in the culture media were measured in a multiplex immunoassay format (Milliplex Map Kit, Millipore) with detection using a Luminex 100™ IS, 200™, or High Throughput System. The lower limit of detection is 3.2 pg/mL with a coefficient of variance $<10\%$. The concentrations of TNF-α and MCP-1 in the culture media were measured using an ELISA kit (R&D Systems) and a microplate reader (Molecular Devices, Sunnyvale, CA, USA), with absorbance detection at 450 nm and correction at 540 or 570 nm. The lower limits of TNF-α and MCP-1 detection by the kits are 23.4 and 15.6 pg/mL, respectively, with a coefficient of variance of $<10\%$.

### 2.10 Statistical analysis

The SPSS package program was used for statistical analyses. Values are expressed as mean ± standard deviation (SD). Differences between two groups were determined using an unpaired Student's *t*-test, and those between multiple groups were evaluated with two-way ANOVA where appropriate. Differences were considered significant at $P < 0.05$.

## 3. Results

### 3.1 Expression of CB1 and CB2 in human monocytes/macrophages

Both freshly isolated human PBMCs, containing monocytes as well as T and B lymphocytes, and THP-a cultured monocytes expressed comparable amount of CB2 and CB1 transcripts (*Figure 1A*). Interestingly, the CB1 and CB2 expression profile was profoundly changed upon induction of differentiation into macrophages. In THP-1 monocytes induced to differentiate by treatment with PMA (up to 10 nM/48 h), both real-time PCR and flow cytometry showed a consistent 8- and 16-fold upregulation of CB1 transcript and surface protein, respectively. The same treatment had the opposite effect on CB2 mRNA expression, decreasing it by $>80\%$ (*Figure 1B* and *C*).

Real-time PCR showed that treatment with PMA also preferentially upregulated CB1 expression in human circulating monocytes. PMA (10 nM for up to 5 days) maximally increased CB1 mRNA expression up to 2- to 3-fold higher than that in undifferentiated monocytes; in contrast, CB2 expression was decreased to $<50\%$ that in untreated monocytes (*Figure 2A*). We found that the CB1:CB2 ratio in freshly isolated human monocytes was 1:17.5 and that in PMA-treated monocyte-derived macrophages was 1:3 (*Figure 2B*).

Because our *in vitro* and *ex vivo* data strongly suggested a significant level of CB1 expression in differentiated human macrophages, we examined the distribution of CB1 in human atheromas. RT–PCR confirmed that human atheromatous plaques, dissected from coronary arteries, strongly expressed both CB1 and CB2 mRNA (*Figure 2C*). Immunohistochemical staining showed that CB1 protein was present in the macrophage-rich area, most of which was found to be co-localized with CD68(+) and CD36(+) macrophages (*Figure 2D* and *E*). We also confirmed that CD68(+) macrophages express CB2, too (*Figure 2E*).

### 3.2 Agonist-stimulated CB1 activity induces reactive oxygen species generation in macrophages

RT–PCR showed that several organs in mice, including brain, liver, and muscle, express CB1 mRNA *in vivo*. Aorta, fat, heart, and lung also express CB1 mRNA, but to a lesser degree (data not shown). Intraperitoneal monocytes/macrophages expressed both CB1 and CB2 (CB1≪CB2) mRNAs under basal conditions. Interestingly, provoking a systemic inflammation by injecting thioglycollate intraperitoneally profoundly decreased CB1 mRNA expression to the nearly undetectable levels in peritoneal macrophages (*Figure 3A*) and in all organs except the brain (data not shown). By injecting thioglycollate into CB2-KO mice, we were able to downregulate CB1 in peritoneal macrophages in the context of genetic ablation of CB2, thus generating a $CB1_{null}$/CB2(−) macrophage model. In contrast, the RAW264.7 mouse macrophage cell line strongly expresses both CB1 and CB2 (*Figure 3A*), and was therefore used in subsequent experiments as a CB1(+)/CB2(+) macrophage model.

RAW264.7 cells labelled with the fluorescent ROS indicator, $H_2$DCFDA, and treated for 30 min with 1 μM AEA, a non-specific agonist of both CB1 and CB2, exhibited a transient increase in fluorescence (*Figure 3B*). Pre-incubation for 1 h with the specific CB1 inhibitor, SR141716 (1 μM), completely abolished this increase in intracellular ROS, suggesting that CB1 mediates ROS generation in macrophages. This interpretation was confirmed by experiments using the highly specific CB1 agonist, ACEA (1 μM), which induced a significant increase in macrophage ROS that was inhibited by pre-treatment with SR141716. In contrast, a 30 min exposure to JWH015 (100 nM), a specific CB2

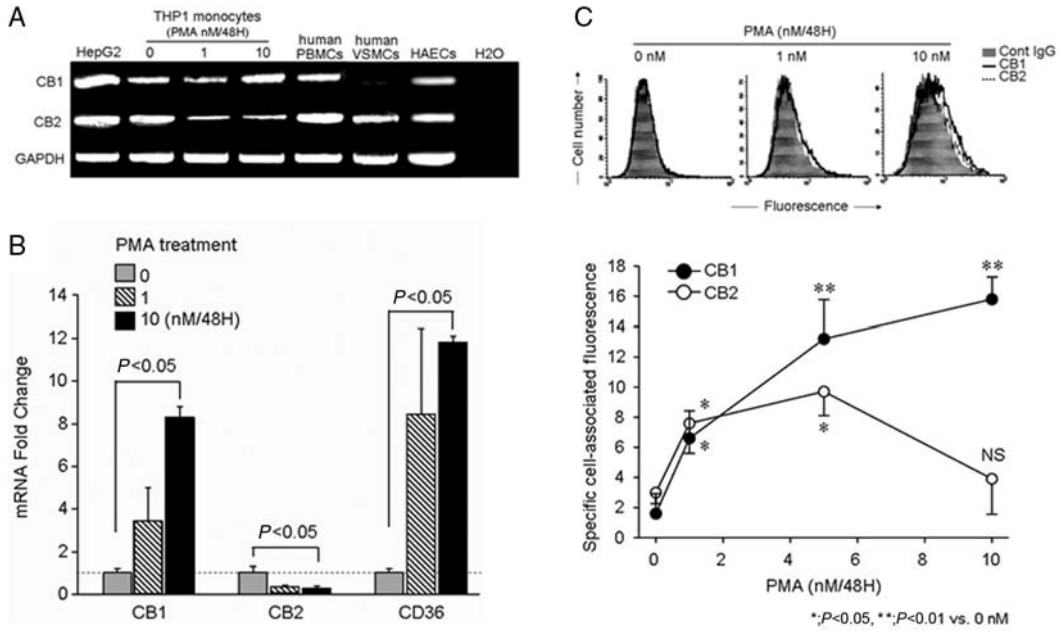


**Figure 1** Expression of CB1 and CB2 in monocytes/macrophages and other cells. mRNA expression levels in the THP-1 monocytic cell line, human vascular smooth muscle cells (VSMCs), and human aortic endothelial cells (HAECs) were estimated by RT–PCR (*A*) and real-time PCR (*B*). The level of surface CB1 protein expression in THP-1 monocytes was estimated by flow cytometry (*C*). Differentiation of monocytes into macrophages was induced by treatment with PMA (1–10 nM) for 48 h. Data represent means ± SD values from three independent experiments performed in triplicate. (B) $P < 0.05$; ANOVA. (C) $^{*}P < 0.05$, $^{**}P < 0.01$; unpaired Student's *t*-test.

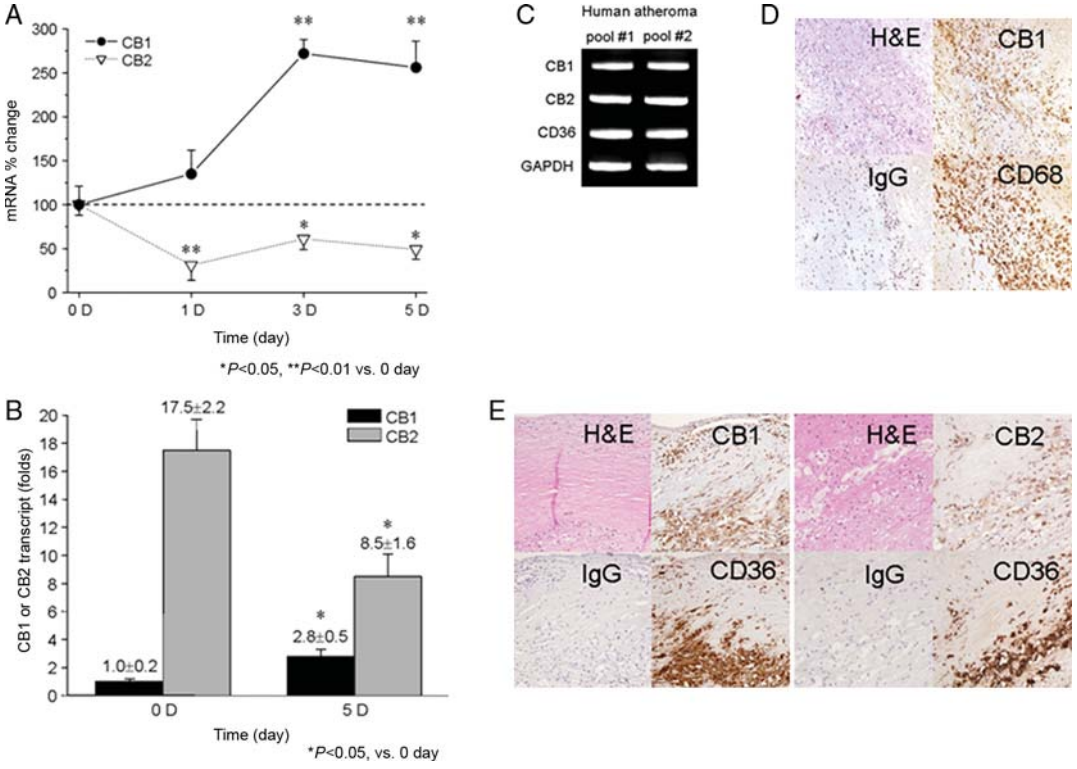


**Figure 2** Expression of CB1 in human monocytes/macrophages and atherosclerotic plaques. (*A*) Human monocytes were freshly isolated from whole blood and cultured for up to 5 days in the presence of 10 nM PMA. Fold changes in CB1 and CB2 mRNA expression (means ± SD) were estimated by real-time PCR. $^{*}P < 0.05$, $^{**}P < 0.01$; unpaired Student's *t*-test. (*B*) Freshly isolated human monocytes were prepared as described in (A). CB1 and CB2 mRNA expression level was estimated by real-time PCR. The standard curve of CB1 and CB2 transcript was obtained by simultaneously amplificating a given number of copies of a vector encoding CB1 or CB2 and the relative amount of CB1 and CB2 transcripts in the sample was calculated. Data represent means ± SD of fold changes. Three independent experiments were performed in triplicate. $^{*}P < 0.05$ vs. 0 day; unpaired Student's *t*-test. (*C*) Atheromas ($n = 6$) dissected from human coronary arteries from three subjects were pooled and used to isolated RNA for RT–PCR. (*D*) Human atheromas prepared as described in (C) were stained with monoclonal IgG antibodies that detect human CB1 and CD68, specific markers for macrophages. Tissues were lightly stained with haematoxylin (H&E) for histology or labelled with isotype-matched IgG (IgG) for negative controls. The figure is representative of six independent samples. (*E*) The distribution of CB1 and CB2 together with CD36 in the human atheroma was estimated by immunohistochemical staining as described in (D) using specific antibodies.

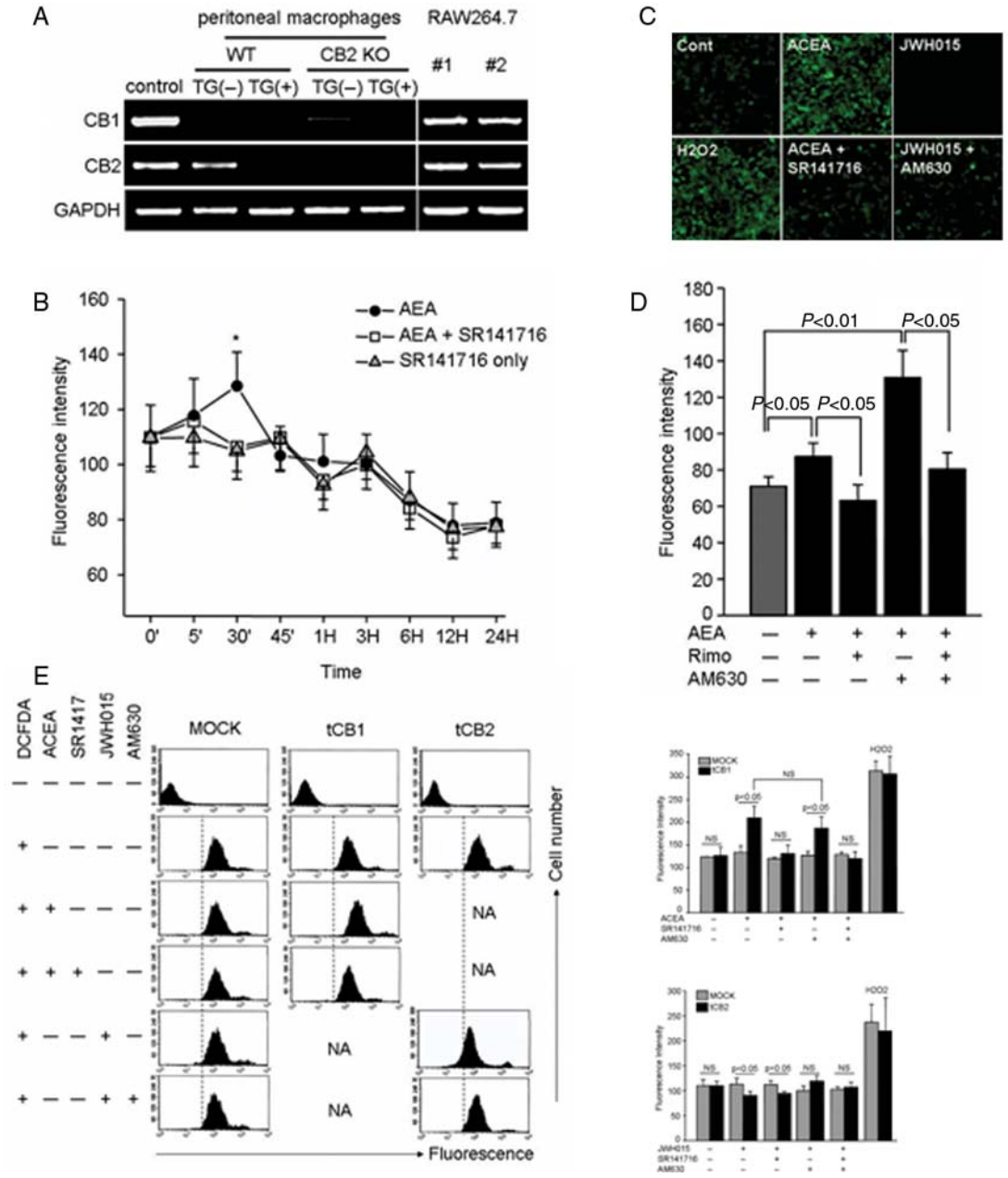


**Figure 3** Reactive oxygen species generation by RAW264.7 cells and thioglycollate-elicited murine intraperitoneal macrophages. (*A*) Thioglycollate (TG) was intraperitoneally injected into CB2–KO (KO) or wild-type (WT) mice. The macrophages were harvested and prepared 3 days after the injection, and CB1 and CB2 mRNAs were detected by RT–PCR. Parallel experiments were performed using elicited peritoneal macrophages from CB2-KO mice transfected with CB1 or CB2. RAW264.7, a cultured mouse macrophage cell line, was analysed as well. The results from elicited peritoneal macrophages are representative of those from three independent experiments. (*B*) RAW264.7 cells were stimulated with the non-selective CB1/CB2 agonist, AEA (1 μM for up to 24 h), with or without selective CB1 blockade with SR141716 (1 μM), and labelled with $H_2$DCFDA (5 μM for 15 min). Cell-associated fluorescence was measured by flow cytometry. Data represent means ± SD of the percent change in fluorescence intensity. Three independent experiments were performed in triplicate. $^*P < 0.05$; unpaired Student's *t*-test. (*C*) $H_2$DCFDA-labelled RAW264.7 cells were stimulated with ACEA (1 μM) or JWH015 (100 nM) for 30 min and then cell-associated fluorescence was visualized using confocal microscopy. The cells were pre-treated with SR141716 (1 μM) or AM630 (300 nM) for 1 h prior to the experiment to block CB1 and CB2, respectively. (*D*) RAW264.7 cells were stimulated with AEA (1 μM for 30 min) in the presence or absence of SR141716 or AM630, labelled with $H_2$DCFDA, and then cell-associated fluorescence was measured by flow cytometry. Data represent means ± SD of fluorescence intensity. Three independent experiments were performed in triplicate. $^*P < 0.05$; unpaired Student's *t*-test. (*E*) Elicited peritoneal macrophages were isolated from thioglycollate-injected CB2-KO mice and then transfected with expression constructs for CB1 (tCB1) or CB2 (tCB2). Mock (MOCK) transfected cells were used as a negative control. The cells were prepared as described in (C), and cell-associated fluorescence was measured by flow cytometry. Three independent experiments were performed in triplicate. Data in the bar graphs represent the means ± SD of the percent change in fluorescence intensity. NS, non-significant; unpaired Student's *t*-test.

activator, tended to reduce $H_2$DCFDA-specific fluorescence, an effect that was blocked by pre-treatment (1 h) with the CB2 inhibitor, AM630 (300 nM) (*Figure 3C*). In RAW264.7 cells, AEA (10 μM)-induced generation of intracellular ROS was potentiated by prior inhibition of CB2 with AM630 (*Figure 3D*), suggesting that CB2 signalling may negatively regulate CB1-stimulated ROS generation.

To confirm that CB1 and CB2 differentially regulate intracellular ROS, we transfected thioglycollate-elicited $CB1_{null}$/CB2(−) murine peritoneal macrophages isolated from

CB2-KO mice with an expression vector encoding either human CB1 or CB2, and quantified changes in intracellular ROS in response to treatment (30 min) with ACEA (1 μM) or JWH015 (100 nM) by flow cytometry. As expected, ACEA only induced ROS generation in elicited peritoneal macrophages transfected with CB1. In contrast, JWH015 treatment induced a small (∼10%), but significant, reduction in intracellular ROS in elicited peritoneal macrophages transfected with CB2 (*Figure 3E*).

### 3.3 CB1-induced reactive oxygen species generation is dependent on the p38-MAPK pathway

To study the signalling pathway involved in CB1-mediated ROS generation, we estimated the degree of ACEA-induced ROS generation in RAW264.7 cells treated with the MEK1 inhibitor, PD98059 (20 μM); the p38-MAPK inhibitor, SB203580 (10 μM), the NF-κB inhibitor, pyrrolidine dithiocarbamate (PDTC,100 μM); the JNK inhibitor, SP600125 (10 μM); or the CB1 inhibitor, SR141716 (1 μM). Only SB203580 as well as SR141716 resulted in complete inhibition of ACEA-induced ROS generation (*Figure 4A*). Immunoblotting also confirmed that p38-MAPK was activated in ACEA-treated, but not JWH015-treated, RAW264.7 cells. And the p38-MAPK was not activated by ACEA (1 μM) in thioglycollate-elicited $CB1_{null}$/CB2(−) murine peritoneal macrophages unless CB1 protein is exogenously expressed (*Figure 4B*).

### 3.4 CB2-activated Rap1 negatively regulates CB1-induced reactive oxygen species generation

Signalling by Rap1, a small G protein of the Ras family, is known to be involved in the suppression of ROS generation[15,16] and the promotion of CB1-mediated neurite outgrowth.[17] To investigate the role of Rap1 CB1-mediate ROS generation in macrophages, we disrupted endogenous Rap1 by transfecting cells with Rap1DN, a dominant negative form of Rap1 (*Figure 5A*). Functional inhibition of Rap1 increased the magnitude of ROS production in response to AEA (1 μM/30 min) in RAW264.7 cells (*Figure 5B*). The potentiation of AEA-stimulated ROS production in Rap1DN-transfected macrophages was recovered by co-transfection with Rap1, proving the role of Rap1 on the suppression of ROS production (*Figure 5B*). Pull-down assays in elicited $CB1_{null}$/CB2(−) murine peritoneal macrophages transfected with either CB1 or CB2 and stimulated with specific agonists for the respective receptors clearly showed that both CB1 and CB2 are responsible for Rap1 activation (*Figure 5C*). Moreover, the ablation of Rap1 in CB1-transfected $CB1_{null}$/CB2(−) murine peritoneal macrophages enhanced AEA-stimulated (1 μM/30 min) ROS generation, confirming that Rap1 activated through CB1 signalling negatively regulates CB1-mediated ROS production. Co-expression of CB2 in those CB1-transfected peritoneal macrophages (i.e. CB1(+)/CB2(+) state) reduced the magnitude of AEA-stimulated ROS generation and additional inhibition of Rap1 increased the magnitude of AEA-stimulated ROS generation, indicating that Rap1, which can be activated by either CB1 or CB2, directly suppresses CB1-stimulated ROS generation in macrophages (*Figure 5D*).

### 3.5 Agonist-stimulated CB1 activity induces TNF-α and MCP-1 production by macrophages

To evaluate ACEA-induced production of TNF-α, MCP-1, IFNγ, IL-1α, IL-6, and IL-12 by elicited CB1(+)/CB2(−)

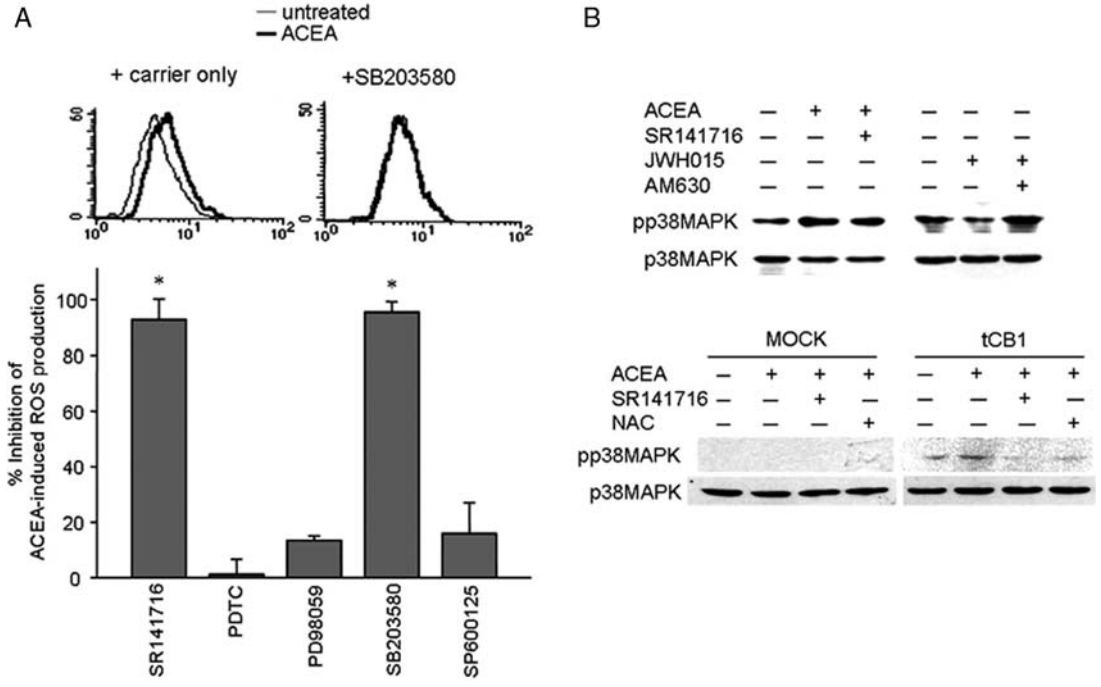


**Figure 4** Involvement of p38-MAPK in CB1-stimulated reactive oxygen species production in macrophages. (*A*) Intracellular ROS generation in ACEA-treated RAW264.7 cells was estimated by flow cytometry, as described in the legend for *Figure 3B*. Prior to stimulation, cells were pre-incubated for 1 h with SR141716 (1 μM), PDTC (100 μM), PD98059 (20 μM), SB203580 (10 μM), or SP600125 (10 μM). Three independent experiments were performed in triplicate. Data in bar graphs represent means ± SD of the percent inhibition of ACEA-induced ROS generation. *$P < 0.05$; unpaired Student's *t*-test. (*B*) RAW264.7 cells (left) or elicited peritoneal macrophages isolated from thioglycollate-injected CB2-KO mice (right) were treated with ACEA (1 μM) or JWH015 (100 nM) for 30 min, and total and phospho-p38-MAPK protein was detected by immunoblotting. The cells were pre-incubated with SR141716 (1 μM), AM630 (300 nM), or NAC (10 mM) for 1 h prior to stimulation. The figure is representative of three independent experiments.

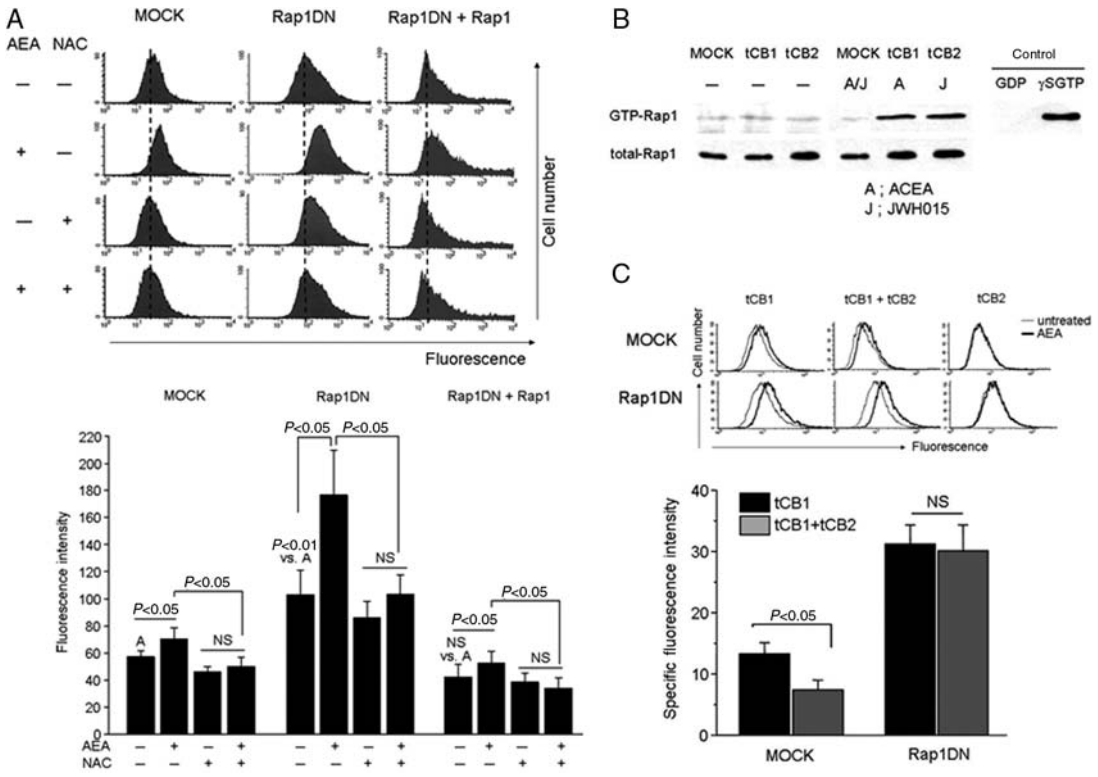


**Figure 5** Effect of macrophage Rap1 on ROS regulation by CB1 and CB2. (*A*) AEA-induced intracellular ROS generation was quantified in $H_2$DCFDA-labelled RAW264.7 cells transfected with dominant-negative Rap1 (Rap1DN), using flow cytometry as described in the *Figure 3B*. Mock-transfected (MOCK) RAW264.7 cells were used as a control. Rap1 was co-transfected to Rap1DN-transfected cells to confirm the specific activity of Rap1DN. Cells were pre-incubated with 10 mM N-acetyl cysteine (NAC) to block oxygen radical generation. Three independent experiments were performed in triplicate. Data in bar graphs represent means ± SD of cell-associated fluorescence intensity. $P < 0.05$, $P < 0.01$, and NS, non-significant; unpaired Student's *t*-test. (*B*) Elicited mouse peritoneal macrophages were isolated from thioglycollate-injected CB2-KO mice and then transfected with expression constructs for CB1 (tCB1) or CB2 (tCB2). Mock-transfected cells (MOCK) served as a negative control. Cells were stimulated with either 1 μM ACEA (A) or 100 nM JWH015 (J) for 10 min, and then pull-down assays were performed to detect the active, GTP-bound form of Rap1. Parallel experiments were performed in the presence of GDP or γSGTP as negative and positive controls, respectively. (*C*) Elicited mouse peritoneal macrophages were isolated from thioglycollate-injected CB2-KO mice and then transfected with expression constructs for CB1 (tCB1), CB2 (tCB2) and/or Rap1DN. Mock-transfected cells (MOCK) served as a negative control. Intracellular ROS generation induced by AEA (1 μM for 30 min) was measured by flow cytometry, as described in the legend for *Figure 3B*. Three independent experiments were performed in triplicate. Data in bar graphs represent means ± SD of cell-associated fluorescence intensity. NS, non-significant; unpaired Student's *t*-test.

murine peritoneal macrophages, we performed a multiplex immunoassay, which showed the elevation of TNF-α and MCP-1 concentrations after 16 h (data not shown). This finding was clearly confirmed by ELISA, which showed that ACEA (1 μM for 16 h) induced a 1.5- to 2-fold increase in TNF-α and MCP-1 in elicited CB1-transfected $CB1_{null}$/CB2(−) murine peritoneal macrophages (*Figure 6A* and *B*). As expected, the p38-MAPK inhibitor, SB203580, together with SR141716 nearly completely abolished ACEA-induced production of TNF-α and MCP-1. Moreover, TNF-α production was inhibited by PDTC (100 μM), and MCP-1 production was inhibited by PDTC (100 μM) and PD98059 (20 μM), confirming that NF-κB and MEK are activated by ROS and are involved in the production of TNF-α and MCP-1.

## 4. Discussion

The present study provides clear evidence that the profile of CB1 expression in monocytes/macrophages depends on species and the degree of differentiation, and relatively high expression of CB1 in human macrophages directly modulates inflammatory activities through ROS production. As confirmed in our study, the predominance of CB2 in naïve monocytes may result in circulating monocytes being 'preset' to exert a more anti-inflammatory response, such as inhibition of chemotactic movement in response to MCP-1[18] and RANTES,[19] when stimulated by cannabinoids. Our study also confirmed that CB1 expression in macrophages in the *in vivo* mouse model is also negligible under the inflammatory conditions. In a previous study, CB2 protein in immunostained atherosclerotic lesions from apoE KO mice was clearly localized to macrophages, but CB1 was not detected.[7] Therefore, CB1 may play little or no role in activating undifferentiated circulating monocytes in human, and macrophages under inflammatory conditions in the murine model.

Unlike murine macrophages, human macrophages display profound CB1 upregulation in response to pro-inflammatory and pro-atherogenic stimuli. Our real-time PCR results clearly showed that the CB1 mRNA expression level in human monocytes, which was only 5% that of CB2, was significantly increased up to one-third of CB2 following exposure to PMA, a potent inducer of differentiation. A previous study also identified other inflammatory mediators, i.e. oxidized LDL and GM-CSF, as positive regulators of monocyte CB1.[20] The substantial expression of CB1 and CB2 protein by human macrophages in the vulnerable plaque *in vivo*, as proved by immunohistochemical staining in our and previous study,[20] leads to a hypothesis that the overall functional outcome of cannabinoid stimulation of intra-plaque macrophages can be

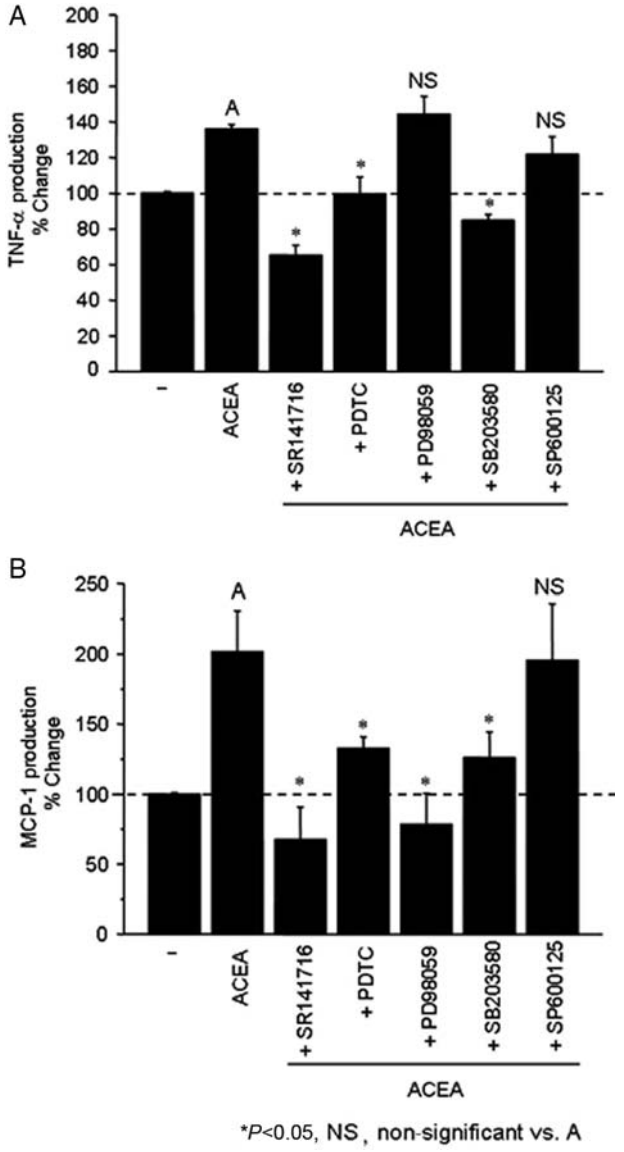


**Figure 6** Signalling pathways involved in mediating CB1-stimulated production of TNF-α and MCP-1 in macrophages. Elicited mouse peritoneal macrophages were isolated from thioglycollate-injected CB2-KO mice and then transfected with an expression construct for CB1. Transfected cells ($2 \times 10^4$ cells/plate) were stimulated with ACEA (1 μM) in the presence or absence of SR141716 (1 μM), PDTC (100 μM), PD98059 (20 μM), SB203580 (10 μM), or SP600125 (10 μM) for 16 h. The concentrations of TNF-α and MCP-1 in the culture media were measured by ELISA. Three independent experiments were performed in triplicate. Data in bar graphs represent means ± SD of the percent change in cytokine concentration. $^*P < 0.05$, NS, non-significant; unpaired Student's *t*-test.

determined by the activation of CB1 as well as CB2. For example, THC, a non-selective cannabinoid receptor agonist, undoubtedly reduces inflammation in the arterial wall in the CB2-predominent murine model.[7] On the other hand, previous human studies have shown that habitual inhalation of THC induces an 8- to 10-fold upregulation of monocyte CB1 mRNA levels and decreases CB2 mRNA expression by 50% compared to that in normal healthy subjects,[21] and not uncommonly induces severe inflammation in peripheral arteries; i.e. obliterative arteritis.[22]

The present study found the novel mechanism by which CB1 activation enhances the pro-inflammatory activities of macrophages. Through exclusive CB1 expression and specific inhibition of CB1 using a highly selective antagonist, SR141716, we proved that CB1 directly induces intracellular ROS generation and p38-MAPK activation by macrophages. The activation of MAP kinases, including p38-MAPK, mediates ROS signalling and induces a number of pro-inflammatory responses.[23] Several studies demonstrated that CB1 induces pro-inflammatory inflammatory responses in various cell lines other than macrophages through MAPK activation.[24–26] The present study clearly describes that such CB1-stimulated ROS generation and p38-MAPK activation triggers pro-inflammatory activities of macrophages, i.e. the production of TNF-α and MCP-1.

The amino acid sequences of CB1 and CB2 show 44% homology.[3] Since CB2 is abundantly co-expressed with CB1 in human macrophages, the influence of CB2 on macrophages should be considered, too. The present study showed that the signalling pathways involving ROS and p38-MAPK were exclusively mediated by CB1 activation in macrophages. Interestingly, the blocking of macrophage CB2 significantly increased the magnitude of CB1-mediated ROS generation in response to AEA. Since CB1 and CB2 compete for binding of non-selective CB agonists like AEA, AEA may bind preferentially to CB1 and generate more ROS if CB2 is pre-occupied by a specific CB2 inhibitor, AM630. However, the potentiating effect of CB2 blockade on CB1-mediated ROS production was consistently observed under conditions in which AEA was present in sufficient excess to saturate CB1, suggesting that agonist-bound CB2 directly generates inhibitory signals and directly suppresses CB1-stimulated ROS production.

We propose that Rap1, a member of the Ras small G protein family, is responsible for the CB2-dependent inhibition of CB1-stimulated ROS production. Interestingly, we found that both CB1 and CB2 could activate Rap1, likely through a common pathway mediated by G(i/o), as described previously.[27,28] We proved that Rap1, activated by either CB1 or CB2, suppressed the CB1-induced generation of intracellular ROS and subsequent pro-inflammatory responses. The outcome of Rap1 signalling is complex and may depend on the specific cell type. The Rap1 activated by CB1 may trigger the outgrowth of neurites through activating pro-inflammatory signallings, such as Src, stat3, Rac1, and JNK pathway that follows Galpha (i/o)/Ral activation.[17] Other previous studies support our findings, in which Rap1 was shown to prevent Ras/Ral-dependent ROS generation in T lymphocytes.[15,16]

The appearance of macrophages/foam cells in the arterial wall undoubtedly facilitates atherogenesis. A previous study showed that the activation of CB1 in the RAW264.7 macrophage cell line upregulated the CD36 scavenger receptor, a macrophage differentiation marker, and promoted cholesterol accumulation.[29] Taken together with our results to show the colocalization of CB1 in CD36(+) macrophages, it is highly possible that upregulated CB1 is not merely a consequence of differentiation, but is also actively involved in facilitating the formation of foam cells. Therefore, the ideal therapeutic approach for reducing the pro-inflammatory activities of macrophages would be to use a selective CB1 antagonist with or without adjunct treatment with a CB2 agonist, rather than to use THC or other non-specific CB agonists.

The benefit of CB1 blockade as a means to prevent atherosclerotic disease has not been demonstrated in humans. However, the results of our study may in part provide

a framework for interpreting the previous finding, in which oral administration of SR14176 reduced the total atheroma volume of human coronary arteries.[30]

**Conflict of interest:** none declared.

## Funding

This work was supported by a grant (M10748000263-07N4800-26310) from the Korea Science and Engineering Foundation (KOSEF) funded by the Korean government (MOST), and also in part by Sanofi-Aventis. K.H.H. and S.L. were supported in part by grants from the Korean Ministry of Health and Welfare (A050020), the Asan Institute for Life Sciences (2009-288), MSD Korea and by the Cardiovascular Research Foundation, Seoul, Korea. This work was also in part supported by grant KRF-2005-205-C00058(I00279).

## References

1. Libby P, Ridker PM, Maseri A. Inflammation and atherosclerosis. *Circulation* 2002;**105**:1135–1143.
2. Valente AJ, Rozek MM, Sprague EA, Schwartz CJ. Mechanisms of intimal monocyte-macrophage recruitment. A special role for monocyte chemotactic protein-1. *Circulation* 1992;**86**:III20–III25.
3. Pacher P, Batkai S, Kunos G. The endocannabinoid system as an emerging target of pharmacotherapy. *Pharmacol Rev* 2006;**58**:389–462.
4. Klein TW, Newton C, Larsen K, Lu L, Perkins I, Nong L *et al*. The cannabinoid system and immune modulation. *J Leukoc Biol* 2003;**74**:486–496.
5. Ghosh S, Preet A, Groopman JE, Ganju RK. Cannabinoid receptor CB2 modulates the CXCL12/CXCR4-mediated chemotaxis of T lymphocytes. *Mol Immunol* 2006;**43**:2169–2179.
6. Coopman K, Smith LD, Wright KL, Ward SD. Temporal variation in CB2R levels following T lymphocyte activation: evidence that cannabinoids modulate CXCL12-induced chemotaxis. *Int Immunopharmacol* 2007;**7**:360–371.
7. Steffens S, Veillard NR, Arnaud C, Pelli G, Burger F, Staub C *et al*. Low dose oral cannabinoid therapy reduces progression of atherosclerosis in mice. *Nature* 2005;**434**:782–786.
8. Rajesh M, Mukhopadhyay P, Hasko G, Huffman JW, Mackie K, Pacher P. CB2 cannabinoid receptor agonists attenuate TNF-alpha-induced human vascular smooth muscle cell proliferation and migration. *Br J Pharmacol* 2008;**153**:347–357.
9. Rajesh M, Mukhopadhyay P, Batkai S, Hasko G, Liaudet L, Huffman JW *et al*. CB2-receptor stimulation attenuates TNF-alpha-induced human endothelial cell activation, transendothelial migration of monocytes, and monocyte-endothelial adhesion. *Am J Physiol Heart Circ Physiol* 2007;**293**:H2210–H2218.
10. Steffens S, Mach F. Cannabinoid receptors in atherosclerosis. *Curr Opin Lipidol* 2006;**17**:519–526.
11. Dol-Gleizes F, Paumelle R, Visentin V, Marés AM, Desitter P, Hennuyer N *et al*. Rimonabant, a selective cannabinoid CB1 receptor antagonist, inhibits atherosclerosis in LDL receptor deficient mice. *Arterioscl Thromb Vasc Biol* 2009;**29**:12–18.
12. Moon EY, Pyo S. Elicited peritoneal lipopolysaccharide stimulates Epac1-mediated Rap1/NF-kappaB pathway in Raw 264.7 murine macrophages. *Immunol Lett* 2007;**110**:121–125.
13. Siegmund SV, Qian T, de Minicis S, Harvey-White J, Kunos G, Vinod KY *et al*. The endocannabinoid 2-arachidonoyl glycerol induces death of hepatic stellate cells via mitochondrial reactive oxygen species. *FASEB J* 2007;**21**:2798–2806.
14. Jaramillo M, Olivier M. Hydrogen peroxide induces murine macrophage chemokine gene transcription via extracellular single-regulated kinase and cyclic adenosine 5′-monophosphate(cAMP)-dependent pathways: Involvement of Nf-kB, activator protein 1, and cAMP response element binding protein. *J Immunol* 2002;**169**:7026–7038.
15. Remans PH, Wijbrandts CA, Sanders ME, Toes RE, Breedveld FC, Tak PP *et al*. CTLA-4IG suppresses reactive oxygen species by preventing synovial adherent cell-induced inactivation of Rap1, a Ras family GTPASE mediator of oxidative stress in rheumatoid arthritis T cells. *Arthritis Rheum* 2006;**54**:3135–3143.
16. Remans PH, Gringhuis SI, van Laar JM, Sanders ME, Papendrecht-van der Voort EA, Zwartkruis FJ *et al*. Rap1 signaling is required for suppression of Ras-generated reactive oxygen species and protection against oxidative stress in T lymphocytes. *J Immunol* 2004;**173**:920–931.
17. He JC, Gomes I, Nguyen T, Jayaram G, Ram PT, Devi LA *et al*. The G alpha(o/i)-coupled cannabinoid receptor-mediated neurite outgrowth involves Rap regulation of Src and Stat3. *J Biol Chem* 2005;**280**:33426–33434.
18. Montecucco F, Burger F, Steffens S. CB2 cannabinoid receptor agonist JWH-015 modulates human monocyte migration through defined intracellular signaling pathways. *Am J Physiol Heart Circ Physiol* 2008;**294**:H1145–H1155.
19. Raborn ES, Marciano-Cabral F, Buckley NE, Martin BR, Cabral GA. The cannabinoid delta-9-tetrahydrocannabinol mediates inhibition of macrophage chemotaxis to RANTES/CCL5: linkage to the CB2 receptor. *J Neuroimmune Pharmacol* 2008;**3**:117–129.
20. Sugamura K, Sugiyama S, Nozaki T, Matsuzawa Y, Izumiya Y, Miyata K *et al*. Activated endocannabinoid system in coronary artery disease and antiinflammatory effects of cannabinoid 1 receptor blockade on macrophages. *Circulation* 2008;**119**:28–36.
21. Nong L, Newton C, Cheng Q, Friedman H, Roth MD, Klein TW. Altered cannabinoid receptor mRNA expression in peripheral blood mononuclear cells from marijuana smokers. *J Neuroimmunol* 2002;**127**:169–176.
22. Noel B, Ruf I, Panizzon RG. Cannabis arteritis. *J Am Acad Dermatol* 2008;**58**:S65–S67.
23. Torres M, Forman HJ. Redox signaling and the MAP kinase pathways. *Biofactors* 2003;**17**:287–296.
24. Sanchez C, Galve-Roperh I, Rueda D, Guzman M. Involvement of sphingomyelin hydrolysis and the mitogen-activated protein kinase cascade in the Delta9-tetrahydrocannabinol-induced stimulation of glucose metabolism in primary astrocytes. *Mol Pharmacol* 1998;**54**:834–843.
25. Derkinderen P, Ledent C, Parmentier M, Girault JA. Cannabinoids activate p38 mitogen-activated protein kinases through CB1 receptors in hippocampus. *J Neurochem* 2001;**77**:957–960.
26. Zhang J, Chen C. Endocannabinoid 2-arachidonoylglycerol protects neurons by limiting COX-2 elevation. *J Biol Chem* 2008;**283**:22601–22611.
27. Jordan JD, Carey KD, Stork PJ, Iyengar R. Modulation of rap activity by direct interaction of Galpha(o) with Rap1 GTPase-activating protein. *J Biol Chem* 1999;**274**:21507–21510.
28. Sugiura T, Waku K. 2-Arachidonoylglycerol and the cannabinoid receptors. *Chem Phys Lipids* 2000;**108**:89–106.
29. Jiang LS, Pu J, Han ZH, Hu LH, He B. Role of activated endocannabinoid system in regulation of cellular cholesterol metabolism in macrophages. *Cardiovasc Res* 2009; Epub ahead.
30. Nissen SE, Nicholls SJ, Wolski K, Rodes-cabau J, Cannon CP, Deanfield JE *et al*. Effect of rimonabant on progression of atherosclerosis in patients with abdominal obesity and coronary artery disease: the STRADIVARIUS randomized controlled trial. *JAMA* 2008;**299**:1547–1560.